Fabrication of polyvinyl alcohol-starch controlled release active film incorporated with 2-hydroxypropyl-β-cyclodextrin/lemongrass oil emulsion for large yellow croaker (*Pseudosciaena crocea*) preservation

[1]Wang, J. X., [1]Fan, X. Y., [1]Chen, Z. J., [1,2,3]*Chen, C. W. and [1,2,3]*Xie, J.

[1]*College of Food Science and Technology, Shanghai Ocean University, Shanghai 201306, China*
[2]*Shanghai Engineering Research Center of Aquatic-Product Processing and Preservation, Shanghai 201306, China*
[3]*Laboratory of Quality and Safety Risk Assessment for Aquatic Products on Storage and Preservation (Shanghai), Ministry of Agriculture, Shanghai 201306, China*

Abstract

Polyvinyl alcohol-starch (PVA/ST) active films incorporated with lemongrass oil (LMO) or 2-hydroxypropyl-β-cyclodextrin, and LMO (HP-β-CD/LMO) emulsion were developed in the present work. The effects of LMO or HP-β-CD/LMO emulsion on the properties of films, and their application in large yellow croaker preservation were investigated. The average particle size and the encapsulation efficiency of the HP-β-CD/LMO emulsion were 150.07 nm and 81.32%, respectively. The scanning electron microscopy (SEM) results revealed that HP-β-CD improved the compatibility between PVA and starch, and LMO was well embedded in HP-β-CD. The incorporation of LMO or HP-β-CD/LMO enhanced the water vapour barrier property and flexibility of the film while weakening its mechanical strength. The oxygen barrier property of the film was weakened by the incorporation of LMO and strengthened by HP-β-CD/LMO. The film incorporated with HP-β-CD/LMO exhibited a little weaker antioxidant and antibacterial activities than the film containing LMO owing to their release property. The existence of HP-β-CD postponed the release of LMO from the film into food simulant (10% ethanol). The preservation results demonstrated that the film containing LMO or HP-β-CD/LMO efficiently inhibited the growth of microorganisms and lipid oxidation of fish; and delayed the decomposition of protein and freshness reduction of large yellow croaker. Additionally, the film added with HP-β-CD/LMO exhibited the best protection for fish quality. In other words, the film with the proper release property of active agents contributed to the preservation of aquatic products.

Introduction

Large yellow croaker (*Pseudosciaena crocea*) is one of the four major commercial fishes in China. It is favoured by many consumers for its delicious meat and rich nutritional value. However, large yellow croaker is prone to spoilage during storage due to its high moisture, fat, and nutrient contents (Zhang *et al.*, 2022). Preservation is key to ensuring the stable quality of aquatic products during storage, and realising long-distance sales or off-season trade. Therefore, it is critical to inhibit the spoilage of the large yellow croaker and extend its shelf life (Zong *et al.*, 2022). With consumers' high demand for food safety, the food industry has developed potential preservation technologies to slow down the quality deterioration of food. Packaging is an indispensable part of food, playing a protective role in the process of food storage (Fu *et al.*, 2018).

Nowadays, active packaging technology has been widely developed for the preservation of perishable food (Wang *et al.*, 2022). It can effectively extend the shelf life, improving the sensory properties of food through the interaction between the packaging material, gases in packaging, and food (Wong *et al.*, 2020). Biodegradable packaging materials have received great attention because they can reduce the environmental pollution caused by petroleum-based

---
*Corresponding author.
Email: cwchen@shou.edu.cn ; jxie@shou.edu.cn

plastic materials. The use of environmentally friendly materials is one of the promising way to improve packaging systems (Göksen *et al.*, 2021).

Polyvinyl alcohol/starch (PVA/ST) composite films have been widely studied as "green packaging material" (Panaitescu *et al.*, 2015). Polyvinyl alcohol (PVA) is an excellent degradable packaging material but has strong hydrophilicity. PVA is broadly applied to varieties of industries due to its good film-forming, barrier, and mechanical properties (Rajabinejad *et al.*, 2020). Starch, as a promising natural polysaccharide consisting of amylose and amylopectin, can be adopted to develop biodegradable films. Blending starch with PVA can not only offset the shortcoming of the starch film but also preserve its biodegradability and lower cost simultaneously (Musa and Hameed, 2020). It has been verified that PVA and starch had good compatibility, and PVA/ST film exhibited excellent mechanical and barrier properties (Ahmed *et al.*, 2020). Additionally, PVA/ST antimicrobial or antioxidant-active films have been considerably researched in recent years (Altaf *et al.*, 2021; Bastante *et al.*, 2021; Srikhao *et al.*, 2021). These films exert antibacterial or antioxidant activity by releasing active agents from films to the food surface. Controlled release active film can effectively regulate the release rate of active substances, thus prolonging its action time, and improving its bioavailability and food preservation effect.

Cyclodextrins (CDs) are potential candidates to be applied for the controlled release of active agents (Lavoine *et al.*, 2014), which are cyclic, water-soluble oligosaccharides composed of several D-glucose units (Farahat, 2020). CDs provide a structure with a hydrophilic outer surface and hydrophobic interior cavity (Eleamen *et al.*, 2017). They can interact with hydrophobic bioactive compounds (molecules), and encapsulate them in their cavity to form inclusion complexes. Besides, CDs exhibited attractive results regarding controlled release in various fields (Niazmand and Razavizadeh, 2021; Wang *et al.*, 2021). 2-hydroxypropyl-β-cyclodextrin (HP-β-CD) is a kind of CD with a large hydrophobic cavity (0.70 nm), and can form more stable drug-inclusion complexes due to its high water solubility (Morais *et al.*, 2017). Furthermore, plant essential oils (PEOs) possess strong antibacterial and antioxidant properties (Song *et al.*, 2020). Lemongrass oil (LMO) belongs to the aromatic plant *Cymbopogon citratus*, exerts a variety of bioactivities, and has a pleasant

aroma (Lee *et al.*, 2020). Nonetheless, PEOs have restricted applications due to their high volatility and sensitivity to environmental factors (Martins *et al.*, 2021). LMO encapsulated by CD emulsion can overcome these difficulties (Li *et al.*, 2021). The combination of PEOs and CDs can form biopolymeric emulsions with high food compatibility to improve the sustained release property and stability of EOs, and can inhibit lipid oxidation and microbial reproduction in fish during storage (Xiao *et al.*, 2019; Chen *et al.*, 2020b).

In the present work, the PVA/ST active films added with LMO or HP-β-CD/LMO emulsion were prepared. The effects of LMO or HP-β-CD/LMO emulsion on the properties of the films were investigated, including physical, structural, antioxidant activity, antibacterial activity, and release property. The preservation effects of these films on large yellow croakers packaging were also evaluated.

Materials and methods

Materials

PVA (1799, mw ≈ 75,000 g/mol) was provided by Sinopec Shanghai Petrochemical Co. Ltd. (China). HP-β-CD, glycerol, and cassava starch (17.8% amylose; 82.2% amylopectin; mw ≈ 1.9×10^7 g/mol; water content: 2.29%) were provided by Laptop Instrument Pvt. Ltd. (USA). LMO was supplied by Scentmeds Co. Ltd. (Thailand). 1,1-dphenyl-2-picrylhydrazyl (DPPH) was purchased from Shanghai Macklin Biochemical Co. Ltd. (China). Ethanol, perchloric acid, trichloroacetic acid, thiobarbituric acid, Tween 80, NaCl, and KOH were purchased from Sangon Biotech (Shanghai) Co. Ltd. Trypticase soy broth (TSB) and trypticase soy agar (TSA) were purchased from Qingdao Haibo Biotechnology Co. Ltd.

Preparation of PVA-ST films

HP-β-CD/LMO emulsion was prepared following Hou *et al.* (2021) with some modifications. Specifically, 0.35 g of LMO was dissolved in 35 mL of 5% ethanol solution, and 70 μL of Tween 80 was added as an emulsifier. Next, 2.1 g of HP-β-CD was added to prepare a suspension of HP-β-CD/LMO emulsion. The mixture was treated in the ultrasonic cell disruptor (Nanjing Immanuel, YMNL-150Y, China) at 65 W for 15 min. HP-β-CD/LMO emulsion was obtained after being placed at room temperature for 24 h.

PVA/ST films were prepared by our previous method (Chen *et al*., 2020a) with some adjustments. Briefly, 10% (w/w) PVA aqueous solution was obtained by stirring in a water bath at 95°C for 2 h. Then, 4% (w/w) cassava starch aqueous solution was stirred at 95°C until the starch was gelatinised. Afterward, the PVA solution (50 g) was mixed with

gelatinised starch solution (50 g). Subsequently, 3.75 mL of glycerol was added as a plasticiser into the mixture. This mixture was continuously stirred for 30 min to obtain a homogenous pure film solution (PFS). The preparation of the films incorporated with LMO or HP-β-CD/LMO emulsion is illustrated in Figure 1.
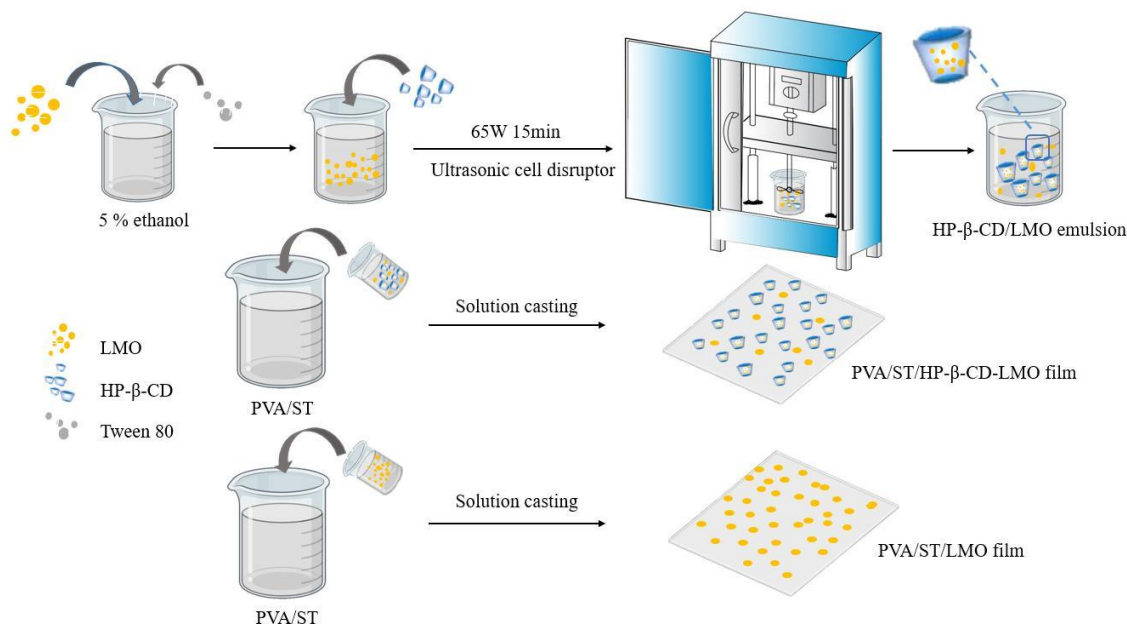
Figure 1. Schematic diagram on the preparation of films incorporated with LMO or HP-β-CD/LMO emulsion.

With the purpose of obtaining PVA/ST film containing LMO (labelled as PVA/ST/LMO), 0.35 g of LMO was dissolved in 35 mL of 5% ethanol solution, and 70 μL of Tween 80 was added as an emulsifier. The mixture was treated in the ultrasonic cell disruptor (Nanjing Immanuel, YMNL-150Y, China) at 65 W for 15 min. Then, it was blended with PFS at 45°C and stirred for 1 h. For PVA/ST film containing HP-β-CD/LMO (labelled as PVA/ST/HP-β-CD-LMO), the prepared HP-β-CD/LMO emulsion was blended with PFS at 45°C and stirred for 1 h. The final solutions were evenly spread on plastic plates, and dried at 40°C for 12 h. The pure PVA/ST film without the addition of LMO or HP-β-CD/LMO emulsion was marked as PVA/ST.

Characterisation of HP-β-CD/LMO emulsion
Particle size distribution

Mastersizer 2000 laser light diffraction instrument (Malvern Instrument, UK) was used to determine the particle size distribution of LMO and HP-β-CD/LMO emulsions. The volume-weighted mean diameter (D [4,3]) was also measured.

Encapsulation efficiency

Following Almasi *et al*. (2020) with some modifications, the encapsulation efficiency (EE) of HP-β-CD/LMO emulsion was determined. Briefly, 1 mL of HP-β-CD/LMO emulsion was diluted with distilled water. The free LMO was then separated by centrifugation at 2,000 rpm for 10 min. The concentration of LMO was determined at 417 nm using a UV-vis spectrophotometer (HITACHI, U-3900, Japan), and calculated using the standard curve constructed in our previous study (Chen *et al*., 2020b). Finally, the EE was calculated using Eq. 1:

$$EE(\%) = \frac{Total\ content\ of\ LMO - Free\ LMO\ content}{Total\ content\ of\ LMO} \times 100\%$$

(Eq. 1)

Characterisation of the active films
Thickness and mechanical properties

A spiral micrometre was used to determine the film thickness by taking six random locations to obtain the average value.

A universal electronic material tester was used to record the tensile strength [TS (MPa)] and

elongation at break [EAB (%)] of the films following ASTM-D882-02. The film samples (150 × 20 mm) were measured under constant temperature and humidity environment (23 ± 1°C, 50 ± 5% RH). Each film was tested six times.

Film colour and transparency

Film colour was indicated by L* (lightness/brightness), a* (redness/greenness), b* (yellowness/blueness), and ΔE (total colour difference). The experiment was carried out according to Chen *et al*. (2020a) using a chroma meter (Konica Minolta, CR-400, Japan). The film sample was placed on a white standard plate ($L_{st}^* = 95.66$; $a_{st}^* = -0.36$; $b_{st}^* = 0.38$) for testing. Film transmittance was measured using a UV-vis spectrophotometer at 280 and 600 nm. The transparency value (TV) was calculated using Eq. 2:

$$\text{TV} = \frac{-logX}{t} \qquad \text{(Eq. 2)}$$

where, t = film thickness, X = transmittance at 280 and 600 nm.

Scanning electron microscopy (SEM)

Film samples were immersed in liquid nitrogen, and fractured immediately (Mahmood *et al*., 2019). The film and fracture surfaces were then sprayed with a layer of gold. SEM (Hitachi SU5000, Japan) was utilised to observe the morphology of the surface and cross-section of all film samples.

Gas barrier property

The water vapour permeability (WVP) tester (Labstone, B-31E, China) was used to determine the WVP of all films at 38°C and 10% RH using the weighing method (GB/T 1037-2021). Film samples were placed on a container with 5 mL of distilled water inside, and it was sealed thoroughly. The result was presented as WVP (g·cm/(cm²·s·Pa)).

The oxygen permeability tester (Mocon, 1/50, USA) was used to measure the oxygen transmission rate (OTR) at 23°C (ASTMD 1434). The carrier and test gases were nitrogen and oxygen, respectively. The result was recorded as OTR (cm³/[m²·day]/0.1 MPa).

LMO release property

The LMO release property was carried out following our previous method (Chen *et al*., 2021) with some modifications. Briefly, 10% ethanol solution (10% Eth) represented an aqueous food, and it was chosen as a food simulant to evaluate the release behaviour of LMO in the films. The film samples (500 mg) were immersed into 100 mL of 10% Eth at 25°C. The amount of LMO in the 500 mg of film samples was determined similarly according to Chen *et al*. (2019). The supernatants were extracted periodically, and examined at 417 nm using a UV-vis spectrophotometer. The content of LMO was calculated based on LMO standard curve using Eq. 3:

$$A_{417} = 1.13277X + 0.00113 \qquad \text{(Eq. 3)}$$

where, A_{417} = absorbance of LMO solution at 417 nm, and X = concentration of LMO in the solution (μL/mL).

Antioxidant activity

DPPH free radical scavenging assay was performed to analyse the antioxidant activity of films following Chenwei *et al*. (2018) with some modifications. Briefly, 1 mL of LMO methanol solution (10.0%, m/v) was mixed with 4 mL of DPPH in methanol (0.1 mM) each. The mixture was placed in the dark at 30°C for 3 h. The absorption was measured at 517 nm (A_{sample}) using a UV-vis spectrometer, and the methanol solution without LMO was used as control ($A_{control}$). The film samples (100 mg) were immersed into 4 mL of DPPH methanol solution (0.1 mM) in the dark at 30°C for 3 h. All the absorption of supernatants was measured at 517 nm (A_{sample}), and pure DPPH methanol solution was used as control ($A_{control}$). Eq. 4 was used to calculate the DPPH radical scavenging rate (Dr):

$$\text{Dr (\%)} = \frac{A_{control} - A_{sample}}{A_{control}} \times 100\% \qquad \text{(Eq. 4)}$$

Antibacterial activity

Shewanella putrefaciens is one of the dominant spoilage bacteria in fresh aquatic products during cold storage. The antibacterial property of the films was characterised by measuring the inhibition rate (IR). *S. putrefaciens* strains were first activated in TSB at 30°C for 24 h. Then they were transferred to the logarithmic growth stage for reserve. The IR of the films was measured according to Chen *et al*. (2020a) with some modifications. The film samples (100 mg) were mixed with 10 mL of the bacterial solution, and they were incubated at 30°C for 12 h. The bacterial solution was diluted to about 10^5 CFU/mL, and 100 μL of the bacterial solution was dispersed onto Petri

dish. TSA was spread all over the dish, and it was incubated at 30°C for 24 h. The blank group was incubated without film samples. Eq. 5 was used to calculate the IR (%):

$$IR\ (\%) = \frac{Count_0 - Count_s}{Count_0} \times 100\% \qquad (Eq.\ 5)$$

where, $Count_0$ = visible colony count of blank group plate, $Count_s$ = visible colony count of experimental group plate.

Preservation of large yellow croaker
Sample treatment

Large yellow croaker (approximately 500 g each) was immediately transported to the laboratory and killed with ice. The back muscles of the fish were promptly cut off, cleaned, and dried. The fish fillets were packaged with three prepared films. Afterward, samples were sealed in polyethylene bags, and stored at 4°C. They were examined at 0, 3, 6, 9, 12, and 15 d to determine the quality of the large yellow croaker, involving total viable count (TVC), thiobarbituric acid reactive substance (TBARS) value, total volatile basic nitrogen (TVB-N), K value, and sensory evaluation. Three parallel experiments were performed for each group.

TVC

The TVC was determined according to Yu *et al.* (2021). Briefly, 5 g of fish samples were mixed with 45 mL of saline solution (0.85% NaCl), and the mixture was homogenised. The homogenate was serially diluted decimally. Next, 1 mL of dilution was injected onto an empty Petri dish, and plate counting agar (PCA) was spread to determine the TVC of the fish sample. All plates were incubated at 37°C for at least 48 h.

TBARS

The TBARS value was determined according to Yıldırım-Yalçın *et al.* (2021) using the aqueous extraction TBA method with slight adjustments. Briefly, 5 g of fish samples were mixed with 25 mL of 20% trichloroacetic acid (TCA) solution. After incubation for 1 h, it was centrifuged at 8,000 rpm and 4°C for 10 min. The supernatant was diluted to 50 mL, and 5 mL of the dilution was transferred to a beaker. Next, 5 mL of TBA solution (0.02 mol/L) were added to the beaker. It was stirred evenly and reacted in a boiling water bath for 20 min. A UV-vis spectrophotometer was used to determine the

absorbance of the solution at 532 nm after it was cooled. 25 mL of TCA solution without fish samples diluted to 50 mL served as the control sample. TBARS values were given as mg MDA/kg.

TVB-N

The TVB-N of fish was determined using the automatic Kjeldahl apparatus (Kjeltec8400, Foss, Denmark) according to Sørensen *et al.* (2020). Briefly, 5 g of shattered fish samples were mixed with 0.5 g of magnesium oxide. The result was expressed as mg N/100 g.

K value

The contents of nucleotides and their metabolites in fish were determined according to Liu *et al.* (2021). Briefly, 2 g of fish were added to 20 mL of 10% perchloric acid solution, the mixture was centrifuged, and the supernatant was removed. Next, 10 mL of 5% perchloric acid solution were mixed with the sediment, which was homogenised and centrifuged. This process was repeated twice, and the supernatants were pooled. KOH solution was used to adjust the pH of the pooled supernatant to 6.4 ~ 6.5. The content of ATP and its metabolites were analysed by high performance liquid chromatography. K value was calculated using Eq. 6:

$$K\ value = \frac{HxR + Hx}{ATP + ADP + AMP + IMP + HxR + Hx} \times 100\%$$
$$(Eq.\ 6)$$

where, ATP, ADP, AMP, IMP, HxR, and Hx = contents of adenosine triphosphate, adenosine diphosphate, adenosine monophosphate, inosine phosphate, hypoxanthine nucleoside, and hypoxanthine, respectively.

Sensory evaluation

Referring to the method of Luan *et al.* (2017) with some modifications, the sensory evaluation of large yellow croaker samples was assessed by a trained 10-member panel (six males and four female between 22 and 45 years old). Samples were randomly taken out, and immediately evaluated by each panellist. Using a 5-point scale, the scoring criteria were as follows: morphology (5, intact; 1, very loose), colour (5, bright; 1, extremely dull), odour (5, extremely desirable; 1, extremely fishy), and elasticity (5, quick rebound after finger pressure; 1, depression after finger pressure). The panellists also rated fresh fish samples as controls.

Statistical analysis

Each test was performed at least three times. For the preservation study of large yellow croaker, three parallel fish samples were tested for each group at the same storage time. The data were processed by the SPSS 22.0 software package. One-way analysis of variance (ANOVA) and Duncan's multiple range tests was used to analyse the experimental data and significant differences ($p < 0.05$).

Results and discussions

Particle size and encapsulation efficiency of HP-β-CD/LMO emulsion

Figure 2 shows the particle size distribution of LMO and HP-β-CD/LMO emulsions. The average particle size of HP-β-CD/LMO emulsion was 150.07 nm, which was smaller than that of the LMO emulsion (231.04 nm). This showed that the addition of HP-β-CD decreased the particle size of the LMO emulsion. This was in agreement with the result that the particle size of CEO nano emulsions decreased following the incorporation of HP-β-CD (Hou *et al.*, 2021). The reason might be that the aggregation of EOs was inhibited due to the inclusion characteristic of HPCD on EOs (Taghi Gharibzahedi *et al.*, 2015).

A high EE value was one of the keys to achieving good controlled release of the encapsulation system (Raeisi *et al.*, 2019). The EE of the HP-β-CD/LMO emulsion was 81.32 ± 2.16%. EOs can be encapsulated in emulsions with HP-β-CD (Hou *et al.*, 2021) since the hydrophilic outer structure and hydrophobic cavity of HP-β-CD enable it to catch hydrophobic compounds into its cavity to form a guest-host inclusion complex (Sun *et al.*, 2021). *Eucalyptus staigeriana* EO has been encapsulated in HP-β-CD to generate lyophilised powder (Yuan *et al.*, 2019a). In our previous study (Chen *et al.*, 2020b), LMO was embedded into β-CD by the co-precipitation method to form the LMO/β-

CD inclusion complex. The EE of the LMO/β-CD inclusion complex was 73.5%, which was lower than that of the HP-β-CD/LMO emulsion in the present work. Therefore, the preparation method in the present work improved the EE of LMO, and simplified the process of film fabrication.
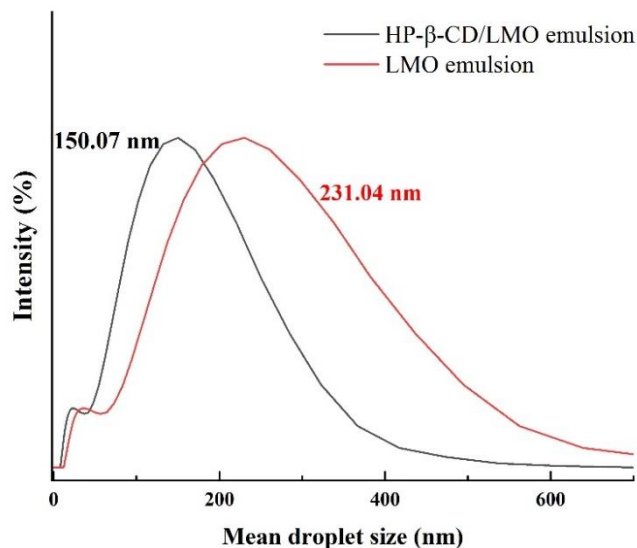
Figure 2. Particle size distribution of LMO and HP-β-CD/LMO emulsions.

Film colour and transparency

Film colour and transparency are listed in Table 1. L* values of all films were around 92 ∼ 93, which indicated high luminance of the films. After adding LMO or HP-β-CD/LMO, the L* values of the films decreased significantly, but there was no significant difference between these two films. There was no notable difference of a* value among the films. However, the b* value of the film increased with the addition of LMO or HP-β-CD/LMO, thus indicating that the film tended to be pale yellow. This was attributed to the light-yellow colour of LMO. The △E value of the films containing LMO or HP-β-CD/LMO did not change significantly, thus indicating that the colour difference between these

Table 1. Colour and transparency of all films.

Film	L*	a*	b*	△E	TV$_{600}$	TV$_{280}$
PVA/ST	93.88 ± 0.52[a]	-0.10 ± 0.08[a]	0.26 ± 0.16[a]	-	0.60 ± 0.11[c]	1.06 ± 0.12[c]
PVA/ST/LMO	92.74 ± 0.29[b]	-0.13 ± 0.01[a]	0.32 ± 0.03[b]	2.98 ± 0.35[a]	0.68 ± 0.05[bc]	2.30 ± 0.25[b]
PVA/ST/HP-β-CD-LMO	92.92 ± 0.34[b]	-0.13 ± 0.02[a]	0.39 ± 0.04[b]	2.79 ± 0.37[a]	0.86 ± 0.01[a]	5.91 ± 0.27[a]

Different lowercase letters in the same column indicate significant differences ($p < 0.05$).

two films was not obvious. Similar result was also reported when adding LMO into cassava starch film (Mendes *et al*., 2020). Several studies suggested that the addition of PEOs could significantly affect the colour of film due to the natural colour of PEOs. For example, Haghighi *et al*. (2019) found that the addition of cinnamon and pink clove EO changed the colour of chitosan-gelatine film evidently. Therefore, the colour of the film added with PEOs depended on the colour of PEOs and its quantity of addition.

When compared with pure PVA/ST film, the TV_{600} value of the films increased with the addition of LMO or HP-β-CD/LMO, and the TV_{600} of PVA/ST/HP-β-CD-LMO film was significantly bigger than that of PVA/ST/LMO film, thus indicating that the transparency of PVA/ST/HP-β-CD-LMO film was relatively poor. This could be attributed to the poor transparency of HP-β-CD, allowing less light to pass through the film. In the ultraviolet spectrum (280 nm), TV_{280} of the film added with LMO or HP-β-CD/LMO was also significantly higher than that of pure PVA/ST film. These results indicated that the presence of LMO improved the UV blocking ability of PVA/ST film and the addition of HP-β-CD/LMO significantly enhanced this ability. Yuan *et al*. (2019b) reported that gelatine film incorporated with hydroxypropyl-β-

CD/morin inclusion complex exhibited good barrier property against UV light.

Mechanical property

Table 2 shows the mechanical property of all films. The film thickness increased slightly by adding LMO or HP-β-CD/LMO. When compared with pure PVA/ST film, the TS of PVA/ST/HP-β-CD-LMO and PVA/ST/LMO films both decreased, while the EAB increased. The decrease in TS was attributed to the increased quantity of voids and oil droplets in the film. This formed discontinuous structures in the film. The stronger polymer-polymer interactions of starch or PVA intermolecular and starch-PVA were partially replaced by weaker PVA-oil or starch-oil interactions in the film network (Atarés and Chiralt, 2016). The plasticising effect of LMO might have led to the increase of EAB, which increased the flexibility and mobility of ST and PVA polymer chains. Similar results were obtained when Javidi *et al*. (2016) added oregano EO into polylactic acid film. When compared with PVA/ST/LMO film, the TS and EAB of PVA/ST/HP-β-CD-LMO film decreased significantly. As shown in the SEM results, this might be attributed to the formation of aggregated particles in the film. This would then form stress concentration points during stretching, thus leading to the weakness of the physical structure of the film.

Table 2. Mechanical and gas barrier properties of all films.

Film	Thickness (mm)	TS (MPa)	EAB (%)	WVP (($\times 10^{-12}$g·cm /(cm2·s·Pa))	OTR (cm³/(m²·24 h·0.1 MPa))
PVA/ST	0.042 ± 0.002[a]	21.5 ± 0.79[a]	125.52 ± 7.62[c]	7.28 ± 0.36[a]	1.25 ± 0.11[a]
PVA/ST/LMO	0.046 ± 0.002[a]	16.5 ± 0.69[b]	155.35 ± 3.68[b]	6.33 ± 0.27[b]	1.86 ± 0.36[b]
PVA/ST/HP-β-CD-LMO	0.052 ± 0.003[b]	10 ± 0.32[c]	139. 62 ± 6.87[a]	6.19 ± 0.38[b]	1.01 ± 0.29[c]

Different lowercase letters in the same column indicate significant differences ($p < 0.05$).

SEM

The surface and cross-section microstructures of all films are shown in Figures 3a - 3f. As observed in Figures 3a and 3d, the surface of the PVA/ST film was not smooth but with some tiny bulges, and the cross-section was rough. These might have been induced by the presence of starch particles, which suggested certain phase separations in the film. Nevertheless, the interface was still indeterminate

between the two parts, thus indicating the strong interactions between PVA and starch. It was consistent with the results reported by Tian *et al*. (2017). When compared with pure PVA/ST film, some small pores and oil drops were found on the surface of PVA/ST/LMO film. There were many small oil drops distributed on the cross-section of the PVA/ST/LMO film. The appearance of pores was attributed to the evaporation or volatilisation of LMO

during film preparation. Similar results were also revealed in the studies about hydroxypropyl methylcellulose-based nanocomposite films added with three kinds of Thai EOs (Klangmuang and Sothornvit, 2016), and gelatine film incorporated with cinnamaldehyde nano emulsions (Ji *et al*., 2021). The surface of the PVA/ST/HP-β-CD-LMO film became smooth except for some aggregation points. Besides, its cross-section was smoother than that of PVA/ST film. This suggested that HP-β-CD

improved the compatibility between PVA and starch. This might be that HP-β-CD was a hydroxypropyl-modified product of β-CD, which had good water solubility, and core material embedding rate. Additionally, sporadic oil droplets were observed on the cross-section of the film, thus implying that LMO was well embedded in HP-β-CD. The disappearance of oil drops and pores on the surface of PVA/ST/HP-β-CD-LMO film showed that LMO was protected by HP-β-CD-LMO effectively during film preparation.
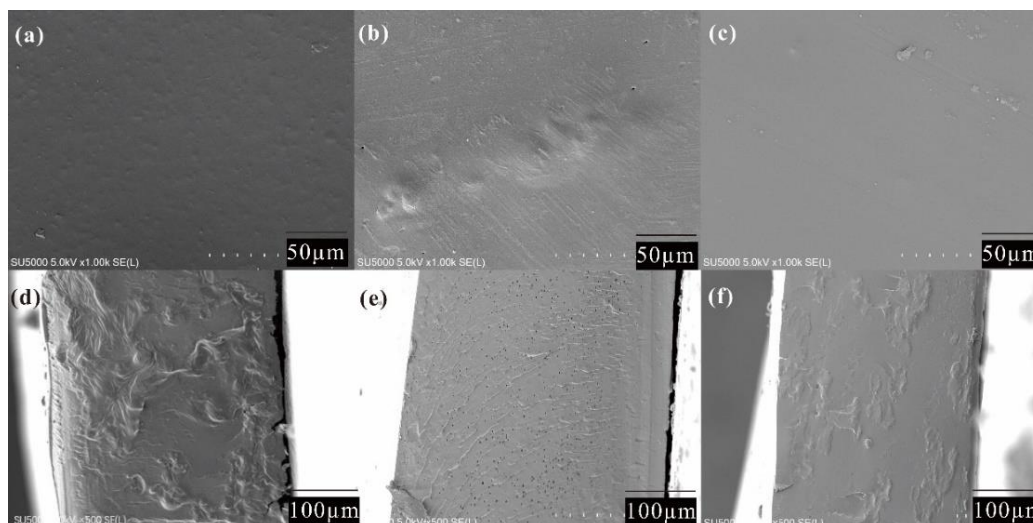
Figure 3. SEM images of the surfaces **(a)** - **(c)** and cross-sections **(d)** - **(f)** of all films: **(a)** and **(d)** = PVA/ST, **(b)** and **(e)** = PVA/ST/LMO, and **(c)** and **(f)** = PVA/ST/HP-β-CD-LMO.

Gas barrier property

The gas barrier properties of all films are summarised in Table 2. The WVP of the films decreased significantly with the incorporation of LMO or HP-β-CD/LMO ($p < 0.05$). The decrease in WVP of PVA/ST/LMO film was due to the hydrophobicity of LMO dispersed in the film, which made water vapour passing through the film more difficult. Similar results were also found when LMO was added into pectin/cassava starch film (Mendes *et al*., 2020), and clove bud EO was incorporated into citrus pectin film (Nisar *et al*., 2018). However, there were some opposite results reported by other studies. For example, an increase in WP was found in gelatine film with the addition of bergamot EO (Ahmad *et al*., 2012). For PVA/ST/HP-β-CD-LMO film, the decrease in WVP was possibly attributed to the decrease in hydrophilicity of the film. This might be due to the hydrogen bonding between HP-β-CD and PVA/ST matrix, and the decrease in OH groups in PVA/ST matrix that could form hydrophilic bonds with water. However, Li *et al*. (2018) found that the WVP of the gelatine film increased with the addition

of thymol EO/β-CD inclusion complex. Therefore, the water vapour barrier ability of the film might rely on comprehensive factors, such as active substance, inclusion compound wall material, and film matrix.

The OTR of the film increased with the addition of LMO since the film structure was affected by the oil droplets and the polymer interaction was weakened, which formed discontinuous and uniform structures. Similar results were mentioned when thyme EO was incorporated into chitosan film (Altiok *et al*., 2010). The OTR of PVA/ST/HP-β-CD–LMO film was significantly lower than that of the other two films. This might be ascribed to the hydrogen interaction between HP-β-CD and PVA/ST matrix that blocked the mobility of PVA and starch chains, thus improving the gas resistance performance. These strong interactions in the polymer-particle interface might also increase the diffusion paths for gas molecules, thus resulting in the enhancement of the gas barrier performance of the film. Therefore, HP-β-CD/LMO emulsion could further enhance the film's resistance to the diffusion of water vapour and oxygen molecules.

Antioxidant activity

The Dr of pure LMO and all films are presented in Figure 4. The Dr of pure PVA/ST film was close to 0, thus suggesting that PVA/ST film exhibited no antioxidant activity. The Dr of PVA/ST/LMO and PVA/ST/HP-β-CD-LMO films were 80.19 ± 0.65 and $75.26 \pm 0.59\%$, respectively, which were higher than the Dr of pure LMO ($69.43 \pm 0.79\%$). This showed that these films had good antioxidant activity. It was ascribed to the antioxidant activity of LMO released from the films. The antioxidant activity was the synergistic action of the main ingredients of LMO, which were citral, myrcene, and geraniol (Majewska *et al.*, 2019). The Dr of PVA/ST/HP-β-CD-LMO film

was a little lower than that of PVA/ST/LMO film. This was attributed to the higher quantity of LMO released from PVA/ST/LMO film than from PVA/ST/HP-β-CD-LMO film for 3 h. This showed that the release rate of LMO slowed down for PVA/ST/HP-β-CD-LMO film. It could be inferred that the action time of the antioxidant activity of PVA/ST/HP-β-CD-LMO film can be extended based on this controlled release property. Yuan *et al.* (2019b) reported that the gelatine film containing HP-β-CD/morin inclusion complex showed controlled release property of morin, which prolonged the action time of the antioxidant activity of the film.
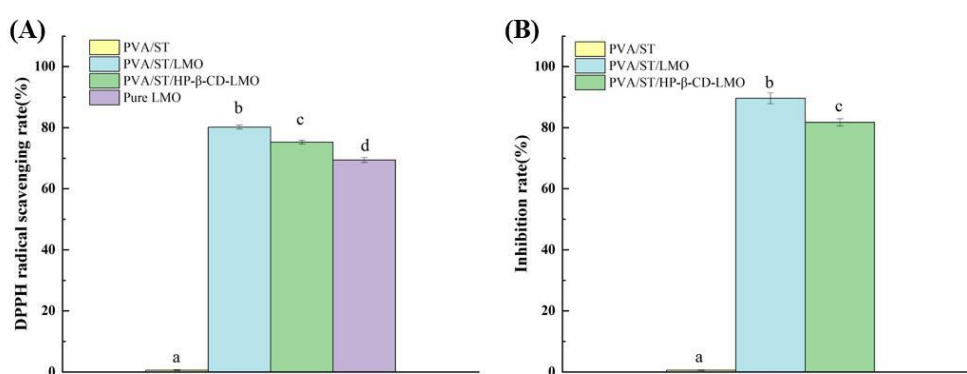
Figure 4. DPPH radical scavenging (%) of pure LMO, PVA/ST, PVA/ST/LMO, and PVA/ST/HP-β-CD-LMO films **(A)**, and inhibition rate (%) of PVA/ST, PVA/ST/LMO, and PVA/ST/HP-β-CD-LMO films **(B)**. Different lowercase letters indicate significant differences ($p < 0.05$).

Antibacterial activity

The IR of all films are presented in Figure 4. The pure PVA/ST film with nearly no IR demonstrated no antimicrobial activity. The IR of PVA/ST/LMO and PVA/ST/HP-β-CD-LMO films were 89.62 ± 1.78 and $81.71 \pm 1.18\%$ respectively, thus indicating their good antimicrobial activity. This can be explained by the fact that the antimicrobial action of LMO released from the films exerted significant antimicrobial effects against *S. putrefaciens*. EOs affected microbial cells through varieties of antimicrobial mechanisms such as destroying enzyme systems, damaging bacterial genetic material, and attacking the phospholipid bilayer of the cell membrane (Abdollahzadeh *et al.*, 2021). The antibacterial properties of LMO depended on its three main components: geranial, neral, and myrcene (Majewska *et al.*, 2019). The antibacterial activity of LMO was assessed through the interactions between its main components and bacterial cell membrane. The lipophilic terpenes

modified the permeability of the cell membrane or changed the intracellular environment (pH and ATP concentrations), thus resulting in cell rupture (Majewska *et al.*, 2019). The IR of PVA/ST/HP-β-CD-LMO film was a little lower when compared with PVA/ST/LMO film. The different release characteristics between PVA/ST/LMO and PVA/ST/HP-β-CD-LMO film contributed to the differences in IR, similar to the reason for the difference in antioxidant activity between the two films.

LMO release property

Releasing curves of LMO from PVA/ST/LMO and PVA/ST/HP-β-CD-LMO films into 10% Eth are shown in Figure 5. Starch and PVA were both typical hydrophilic swelling polymers. The release mechanism of LMO was swelling-induced (Chen *et al.*, 2019). As seen from Figure 5, the two films both underwent three stages: LMO was released rapidly in the early stage, then slowed down, and finally it

reached equilibrium. However, the release of LMO from the films reached equilibrium at 60 h for PVA/ST/LMO film, and at 168 h for PVA/ST/HP-β-CD-LMO film, respectively. This suggested that the film containing HP-β-CD exhibited a slower LMO releasing rate, and took longer to achieve equilibrium. Firstly, when compared with PVA/ST/LMO film, LMO in PVA/ST/HP-β-CD-LMO film need to take some time to move into the film matrix through the hydrophobic cavity of HP-β-CD because HP-β-CD-LMO provided a reservoir for LMO that acted as a core-shell structure of LMO to induce a "lag-time effect". Hou *et al.* (2021) also found the release rate of cinnamon EO in HP-β-CD-added emulsions slowed down significantly. Similar result was obtained by using β-CD to slow down the release of chlorhexidine digluconate (Lavoine *et al.*, 2014). Niazmand and Razavizadeh (2021) also reported the controlled release of bioactive agents (*Ferula asafoetida* leaf and gum extracts) in the polyethylene films, which was in the form of β-CD inclusion complexes. Secondly, the increased thickness, and the improvement of hydrophobicity and water resistance of PVA/ST/HP-β-CD-LMO film reduced the expansion rate of the film to a certain extent, thus retarding the release of LMO. In addition, the content of LMO at equilibrium released from PVA/ST/HP-β-CD-LMO film was a little higher than that of PVA/ST/LMO film. The reason might be that the loss of LMO in PVA/ST/HP-β-CD-LMO film was smaller during film preparation due to the protection of HP-β-CD.
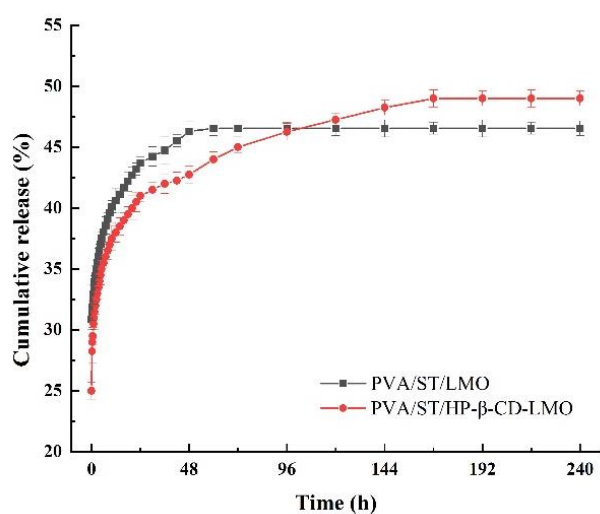
Figure 5. Releasing curves of PVA/ST/LMO and PVA/ST/HP-β-CD-LMO films.

Preservation of large yellow croaker
TVC

Figure 6A shows the change in TVC value of large yellow croaker during storage. The low count (2.4 log CFU/g) of the initial TVC indicated that the large yellow croakers were in good quality. There was an apparent increase in TVC for all samples during storage, thus indicating the quality deterioration of fish fillets. The TVC of fishes packed with the films containing LMO was significantly lower than that of the PVA/ST group ($p < 0.05$). The TVC of the PVA/ST group exceeded 7.0 log CFU/g on day 12, which was defined as the "shelf life" limit (Tao *et al.*, 2019). These indicated that the films containing LMO could retard the reproduction of microorganisms to prolong the shelf life of large yellow croaker. This was ascribed to the antibacterial activity of LMO released from the films to the surface of the fish. EOs acted against microorganisms through varieties of antimicrobial mechanisms, including destroying enzyme systems, damaging bacterial genetic material, and attacking the phospholipid bilayer of the cell membrane (Abdollahzadeh *et al.*, 2021). On the 15th day, the TVC of the PVA/ST/LMO group exceeded 7.0 log CFU/g, while the TVC of the PVA/ST/HP-β-CD-LMO group was still 5.8 log CFU/g. This indicated that PVA/ST/HP-β-CD-LMO film was more beneficial to delay the deterioration of fish quality. This might have been due to the low oxygen permeability of PVA/ST/HP-β-CD-LMO film, which reduced the oxygen in the packaging during storage. It also might be related to the release behaviour of PVA/ST/HP-β-CD-LMO film. When compared with PVA/ST/LMO film, the release rate of LMO released from PVA/ST/HP-β-CD-LMO film slowed down, and the LMO concentration was a little higher at equilibrium. Therefore, it prolonged the action time of LMO to protect the fish from spoilage.

TBARS

Fish are rich in unsaturated fatty acids, which can easily oxidise to produce an undesirable rancid odour. TBA value is an index to evaluate the oxidation degree of secondary lipids, and quantify the degradation of secondary and by-products of polyunsaturated fatty acids, which can be characterised by malondialdehyde (MDA) content (Chu *et al.*, 2022). As shown in Figure 6B, the initial amount of MDA was about 0.04 mg MDA/kg. The TBA of all groups first increased, and then decreased.
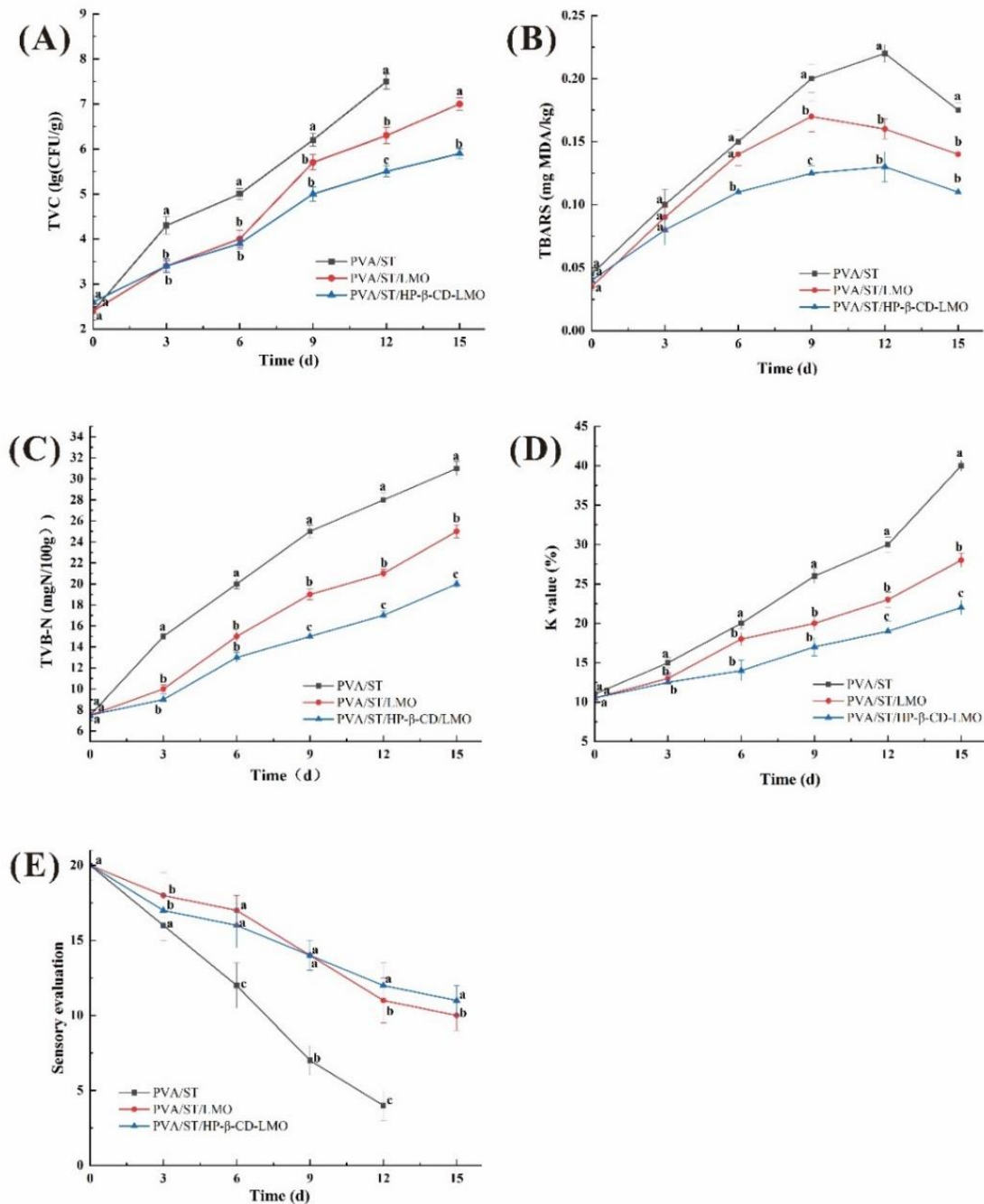
Figure 6. Changes in TVC **(A)**, TBARS **(B)**, TVB-N **(C)**, K value **(D)**, and sensory evaluation **(E)** of large yellow croakers packed by PVA/ST, PVA/ST/LMO, and PVA/ST/HP-β-CD-LMO films during storage at 4°C. Different lowercase letters indicate significant differences among different packaging groups at the same storage time.

When compared with the PVA/ST group, the increasing rate of MDA content of the PVA/ST/LMO and PVA/ST/HP-β-CD-LMO groups was significantly slower ($p < 0.05$). Moreover, the MDA content of the PVA/ST/HP-β-CD-LMO group was always the lowest among the three groups. Hence, the films containing LMO retarded the lipid oxidation of

fish, and the PVA/ST/HP-β-CD-LMO film further enhanced the inhibition degree. This indicated that the films added with LMO displayed good antioxidant activity. The main component of LMO is citral, followed by β-myrcene. The mechanism of antioxidant action of LMO comprised the binding of transition metal ion catalyst, prevention of radical

chain initiation, interaction with the free radicals, and decomposition of peroxides (Perumalla and Hettiarachchy, 2011). The lowest MDA of the PVA/ST/HP-β-CD-LMO group was provoked by the excellent oxygen barrier property of PVA/ST/HP-β-CD-LMO films. The decreasing oxygen content in packaging had a direct effect on delaying the lipid oxidation of fish fillets. Furthermore, the reduction of TBA at the later stage of storage might be derived from the reaction of MDA with free amino acids produced by protein degradation.

TVB-N

Figure 6C shows the TVB-N changes of large yellow croaker during storage. The initial TVB-N value was between 6 - 8 mg N/100 g, thus indicating that the fish was fresh. It could be seen that the TVB-N of all samples increased significantly with increasing in storage time ($p < 0.05$), thus suggesting that the protein of fish degraded into ammonia, amines, and other basic nitrogen-containing substances. This indicated that the activities of spoilage bacteria and the endogenous enzymes were gradually enhanced (Liu *et al*., 2019). Bacterial catabolism of amino acids in fish muscle led to the accumulation of a series of volatile bases such as trimethylamine, dimethylamine, and ammonia, which resulted in the increase in TVB-N (Li *et al*., 2013). When compared with the other two groups, the TVB-N of the PVA/ST group increased faster, and exceeded the upper limit value (30 mgN/100 g) on day 15. The TVB-N of PVA/ST/HP-β-CD-LMO group was 20 mgN/100 g, which was lower than that of PVA/ST/LMO group (25 mgN/100 g). These indicated that the film incorporated with LMO could delay the decomposition of protein and PVA/ST/HP-β-CD-LMO film exhibited the best protective effect. This was ascribed to the antibacterial and antioxidant activities of the film containing LMO (Chen *et al*., 2020a). The released LMO could act on the cell wall and cell membrane systems of spoilage bacteria, thus disrupting their barrier function and preventing them from reproduction. It could also work on enzymes or functional proteins, thus depriving cells of the material basis for growth and reproduction. For the best quality of the PVA/ST/HP-β-CD-LMO group, it might be attributed to the improved gas barrier performance of PVA/ST/HP-β-CD-LMO film. It isolated the entry of oxygen and water vapour, and delayed water loss, thus creating an advantageous environment to protect the protein from

decomposition. In addition, more persistent slow release of LMO and higher release of LMO at the later stage might have improved the duration of LMO efficacy, thus delaying the decline in quality of fish.

K value

Nucleotides are involved in the basic life activities such as heredity, development, and growth. Their critical components are ATP-related compounds. ATP in muscle is degraded into ADP, AMP, IMP, HxR, and Hx after the fish die. IMP gives fish a sweet and meaty taste, while HxR and Hx gives fish a bitter taste (Yang *et al*., 2019). K-value is defined as the percentage of the sum of the end products of the ATP degradation chain (HxR and Hx) to the total of ATP and its degradation products. The K-value is inversely proportional to the freshness of the fish. It could be considered fresh if the K-value is below 20%, and moderately fresh if between 20 and 50% (Lan *et al*., 2021). Changes in K values of fish during storage are presented in Figure 6D. The initial K-value of fish was about 11%, thus suggesting that it was at a very fresh level. This then increased continuously during storage, showing that the freshness of the fish decreased significantly ($p < 0.05$). This meant that the contents of hypoxanthine nucleoside (HxR) and hypoxanthine (Hx) increased significantly after ATP degradation (Yu *et al*., 2021). When compared with PVA/ST group, the K-value of the other two groups increased slower, thus indicating that the LMO-contained films could better inhibit the degradation of ATP. The K value of PVA/ST/HP-β-CD-LMO group was significantly less than that of the PVA/ST/LMO group ($p < 0.05$), thus suggesting that PVA/ST/HP-β-CD-LMO film showed the best protection for the freshness of fish. The reason might be related to the best gas barrier property of PVA/ST/HP-β-CD-LMO film and its release behaviour, which was similar with the analysis discussed earlier in other quality indicators.

Sensory evaluation

The sensory scores of all fish samples during storage are shown in Figure 6E. Sensory profile is an important parameter for fish quality evaluation (Hui *et al*., 2016). The highest score was obtained for all fish samples on 0th day, thus indicating that the fish samples were initially in a high quality. The sensory scores of all groups showed a downward trend. The decreased sensory scores might have been induced by the increase in microbial growth and lipid oxidation

(Lan *et al.*, 2020). The fish samples in PVA/ST group had a slight fishy odour on the 6th day, and the colour became slightly dull. On the 9th day, the texture of fish samples in PVA/ST group became loose and lost elasticity. It also produced a distinct fishy smell. These indicated that the fish's sensory quality was close to unacceptable. The sensory score of PVA/ST group was below 5 on 12th day, which was considered unacceptable to consumers. When compared with PVA/ST group, the sensory scores of other two groups decreased significantly slower throughout the storage period ($p < 0.05$), which suggested that their sensory quality was better than that of PVA/ST group. This may be attributed to fact that microbial propagation and endogenous physicochemical changes of the fish were inhibited by the films added with LMO. In the first nine days, although the sensory scores of PVA/ST/LMO group were slightly higher than that of PVA/ST/HP-β-CD-LMO group, there was no significant difference between them. This indicated that they exhibited similar sensory quality. However, the sensory scores of PVA/ST/HP-β-CD-LMO group exceeded that of PVA/ST/LMO group significantly ($p < 0.05$) after the 9th day, thus showing that the best sensory quality was maintained by PVA/ST/HP-β-CD-LMO film at the end of storage. This was also consistent with the other quality indicators discussed earlier. In addition, the fish samples packed by LMO contained films had a light lemongrass aroma, which was attributed to the odour of the released LMO. By contrast, the odour of lemongrass aroma in PVA/ST/LMO group was a little stronger than that in PVA/ST/HP-β-CD-LMO group. This was due to the inclusion characteristic of HPCD on LMO, which was propitious to weaken the effect of its odour on the sensory quality of fish. On the whole, the odour of lemongrass in the PVA/ST/LMO and PVA/ST/HP-β-CD-LMO group on the sensory quality was acceptable for sensory evaluators.

Conclusion

The PVA/ST active film added with LMO or HP-β-CD/LMO emulsion was successfully developed and characterised. The addition of HP-β-CD reduced the particle size of the LMO emulsion. SEM showed that HP-β-CD improved the compatibility between PVA and starch, and LMO was well embedded in HP-β-CD. The addition of LMO or HP-β-CD/LMO improved the UV-blocking capability, water vapour resistance, and flexibility of film, but weakened its mechanical strength. The incorporation of LMO reduced the oxygen barrier property of the film, while HP-β-CD/LMO improved it. PVA/ST/HP-β-CD/LMO film exhibited a little weaker antioxidant and antibacterial activities than PVA/ST/LMO film, which were related to their release properties. It showed that the existence of HP-β-CD postponed the release of LMO from the film into food simulant. When compared with pure PVA/ST film, PVA/ST/LMO and PVA/ST/HP-β-CD-LMO films could efficiently inhibit the growth of microorganisms and lipid oxidation of fish, which also delayed the decomposition of protein, freshness, and sensory quality reduction of fish. Additionally, PVA/ST/HP-β-CD-LMO film showed the best protection for fish from quality deterioration. The results indicated that the films with proper release property of active agents could be conducive to the preservation of aquatic products.

Acknowledgement

References

Abdollahzadeh, E., Nematollahi, A. and Hosseini, H. 2021. Composition of antimicrobial edible films and methods for assessing their antimicrobial activity: A review. Trends in Food Science and Technology 110(2): 291-303.

Ahmad, M., Benjakul, S., Prodpran, T. and Agustini, T. W. 2012. Physico-mechanical and antimicrobial properties of gelatin film from the skin of unicorn leatherjacket incorporated with essential oils. Food Hydrocolloids 28(1): 189-199.

Ahmed, A., Bilal, M., Niazi, K., Jahan, Z., Samin, G., Pervaiz, E. and Hussain, A. 2020. Enhancing the thermal, mechanical and swelling properties of PVA/starch nanocomposite membranes incorporating-C_3N_4. Journal of Polymers and the Environment 28: 100-115.

Almasi, H., Azizi, S. and Amjadi, S. 2020. Development and characterization of pectin

films activated by nanoemulsion and Pickering emulsion stabilized marjoram (*Origanum majorana* L.) essential oil. Food Hydrocolloids 99(6): 105338.

Altaf, F., Niazi, M. B. K., Jahan, Z., Ahmad, T., Akram, M. A., safdar, A., … and Sher, F. 2021. Synthesis and characterization of PVA/starch hydrogel membranes incorporating essential oils aimed to be used in wound dressing applications. Journal of Polymers and the Environment 29(1): 156-174.

Altiok, D., Altiok, E. and Tihminlioglu, F. 2010. Physical, antibacterial and antioxidant properties of chitosan films incorporated with thyme oil for potential wound healing applications. Journal of Materials Science - Materials in Medicine 21(7): 2227-2236.

Atarés, L. and Chiralt, A. 2016. Essential oils as additives in biodegradable films and coatings for active food packaging. Trends in Food Science and Technology 48: 51-62.

Bastante, C. C., Silva, N. H. C. S., Cardoso, L. C., Serrano, C. M., Martínez de la Ossa, E. J., ... and Vilela, C. 2021. Biobased films of nanocellulose and mango leaf extract for active food packaging: Supercritical impregnation versus solvent casting. Food Hydrocolloids 117(2): 106709.

Chen, C., Li, C., Yang, S., Zhang, Q., Yang, F., Tang, Z. and Xie, J. 2019. Development of new multilayer active packaging films with controlled release property based on polypropylene/poly(vinyl alcohol)/polypropylene incorporated with tea polyphenols. Journal of Food Science 84(7): 1836-1843.

Chen, C., Zong, L., Wang, J. and Xie, J. 2021. Microfibrillated cellulose reinforced starch/polyvinyl alcohol antimicrobial active films with controlled release behavior of cinnamaldehyde. Carbohydrate Polymers 272(4): 118448.

Chen, S., Wu, M., Lu, P., Gao, L., Yan, S. and Wang, S. 2020a. Development of pH indicator and antimicrobial cellulose nanofibre packaging film based on purple sweet potato anthocyanin and oregano essential oil. International Journal of Biological Macromolecules 149: 271-280.

Chen, Z., Zong, L., Chen, C. and Xie, J. 2020b. Development and characterization of PVA-starch active films incorporated with β-

cyclodextrin inclusion complex embedding lemongrass (*Cymbopogon citratus*) oil. Food Packaging and Shelf Life 26(9): 100565.

Chenwei, C., Zhipeng, T., Yarui, M., Weiqiang, Q., Fuxin, Y., Jun, M. and Jing, X. 2018. Physicochemical, microstructural, antioxidant and antimicrobial properties of active packaging films based on poly(vinyl alcohol)/clay nanocomposite incorporated with tea polyphenols. Progress in Organic Coatings 123(7): 176-184.

Chu, Y., Tan, M., Bian, C. and Xie, J. 2022. Effect of ultrasonic thawing on the physicochemical properties, freshness, and protein-related properties of frozen large yellow croaker (*Pseudosciaena crocea*). Journal of Food Science 87(1): 52-67.

Eleamen, G. R. A., Da Costa, S. C., Lima-Neto, R. G., Neves, R. P., Rolim, L. A., Rolim-Neto, P. J. and Oliveira, E. E. 2017. Improvement of solubility and antifungal activity of a new aminothiophene derivative by complexation with 2-hydroxypropyl-β-cyclodextrin. Journal of the Brazilian Chemical Society 28(1): 116-125.

Farahat, M. G. 2020. Enhancement of β-cyclodextrin production and fabrication of edible antimicrobial films incorporated with clove essential oil/β-cyclodextrin inclusion complex. Microbiology and Biotechnology Letters 48(1): 12-23.

Fu, L., Wang, C., Ruan, X., Li, G., Zhao, Y. and Wang, Y. 2018. Preservation of large yellow croaker (*Pseudosciaena crocea*) by Coagulin L1208, a novel bacteriocin produced by *Bacillus coagulans* L1208. International Journal of Food Microbiology 266(5): 60-68.

Göksen, G., Fabra, M. J., Pérez-Cataluña, A., Ekiz, H. I., Sanchez, G. and López-Rubio, A. 2021. Biodegradable active food packaging structures based on hybrid cross-linked electrospun polyvinyl alcohol fibers containing essential oils and their application in the preservation of chicken breast fillets. Food Packaging and Shelf Life 27(6): 100613.

Haghighi, H., Biard, S., Bigi, F., De Leo, R., Bedin, E., Pfeifer, F. and Pulverenti, A. 2019. Comprehensive characterization of active chitosan-gelatin blend films enriched with different essential oils. Food Hydrocolloids 95(2): 33-42.

Hou, K., Xu, Y., Cen, K., Gao, C., Feng, X. and Tang, X. 2021. Nanoemulsion of cinnamon essential oil co-emulsified with hydroxypropyl-β-cyclodextrin and tween-80: Antibacterial activity, stability and slow release performance. Food Bioscience 43(3): 101232.

Hui, G., Liu, W., Feng, H., Li, J. and Gao, Y. 2016. Effects of chitosan combined with nisin treatment on storage quality of large yellow croaker (*Pseudosciaena crocea*). Food Chemistry 203: 276-282.

Javidi, Z., Hosseini, S. F. and Rezaei, M. 2016. Development of flexible bactericidal films based on poly(lactic acid) and essential oil and its effectiveness to reduce microbial growth of refrigerated rainbow trout. LWT - Food Science and Technology 72: 251-260.

Ji, M., Wu, J., Sun, X., Guo, X., Zhu, W., Li, Q., ... and Wang, S. 2021. Physical properties and bioactivities of fish gelatin films incorporated with cinnamaldehyde-loaded nanoemulsions and vitamin C. LWT - Food Science and Technology 135(5): 110-103.

Klangmuang, P. and Sothornvit, R. 2016. Barrier properties, mechanical properties and antimicrobial activity of hydroxypropyl methylcellulose-based nanocomposite films incorporated with Thai essential oils. Food Hydrocolloids 61: 609-616.

Lan, W. Q., Liu, L., Zhang, N. N., Huang, X., Weng, Z. M. and Xie, J. 2020. Effects of ε-polylysine and rosemary extract on the quality of large yellow croaker (*Pseudosciaena crocea*) stored on ice at 4 ± 1°C. Journal of Food Biochemistry 44(10): 1-11.

Lan, W., Zhao, X., Wang, M. and Xie, J. 2021. Effects of chitosan and apple polyphenol coating on quality and microbial composition of large yellow croaker (*Pseudosciaena crocea*) during ice storage. Journal of the Science of Food and Agriculture 102(8): 3099-3106.

Lavoine, N., Tabary, N., Desloges, I., Martel, B. and Bras, J. 2014. Controlled release of chlorhexidine digluconate using β-cyclodextrin and microfibrillated cellulose. Colloids and Surfaces B - Biointerfaces 121: 196-205.

Lee, J. E., Seo, S. M., Huh, M. J., Lee, S. C. and Park, I. K. 2020. Reactive oxygen species mediated-antifungal activity of cinnamon bark (*Cinnamomum verum*) and lemongrass (*Cymbopogon citratus*) essential oils and their constituents against two phytopathogenic fungi. Pesticide Biochemistry and Physiology 168(4): 104644.

Li, B., Wang, X., Gao, X., Ma, X., Zhang, L., Mei, J. and Xie, J. 2021. Shelf-life extension of large yellow croaker (*Larimichthys crocea*) using active coatings containing lemon verbena (*Lippa citriodora* Kunth.) essential oil. Frontiers in Nutrition 8(7): 1-14.

Li, M., Zhang, F., Liu, Z., Guo, X., Wu, Q. and Qiao, L. 2018. Controlled release system by active gelatin film incorporated with β-cyclodextrin-thymol inclusion complexes. Food and Bioprocess Technology 11(9): 1695-1702.

Li, T., Li, J. and Hu, W. 2013. Changes in microbiological, physicochemical and muscle proteins of post mortem large yellow croaker (*Pseudosciaena crocea*). Food Control 34(2): 514-520.

Liu, W., Mei, J. and Xie, J. 2021. Effect of locust bean gum-sodium alginate coatings incorporated with daphnetin emulsions on the quality of *Scophthalmus maximus* at refrigerated condition. International Journal of Biological Macromolecules 170: 129-139.

Liu, X., Xiong, G., Wang, X., Shi, L., Jiao, C., Wu, W. and Wang, L. 2019. Quality changes of prepared weever (*Micropterus salmoides*) by base trehalose solution during repeated freeze-thaw cycles. Journal of Food Processing and Preservation 43(10): e14117.

Luan, L., Fu, S., Yuan, C., Ishimura, G., Chen, S., Chen, J. and Hu, Y. 2017. Combined effect of superchilling and tea polyphenols on the preservation quality of hairtail (*Trichiurus haumela*). International Journal of Food Properties 20(5): S992-S1001.

Mahmood, K., Kamilah, H., Sudesh, K., Karim, A. A. and Ariffin, F. 2019. Study of electrospun fish gelatin nanofilms from benign organic acids as solvents. Food Packaging and Shelf Life 19(7): 66-75.

Majewska, E., Kozlowska, M., Gruczynska-Sekowska, E., Kowalska, D. and Tarnowska, K. 2019. Lemongrass (*Cymbopogon citratus*) essential oil: Extraction, composition, bioactivity and uses for food preservation - A review. Polish Journal of Food and Nutrition Sciences 69(4): 327-341.

Martins, W. D. S., de Araújo, J. S. F., Feitosa, B. F., Oliveira, J. R., Kotzebue, L. R. V., Agostini, D. L. D. S., … and da Silva, A. L. 2021. Lemongrass (*Cymbopogon citratus* DC. Stapf) essential oil microparticles: Development, characterization, and antioxidant potential. Food Chemistry 355(12): 129644.

Mendes, J. F., Norcino, L. B., Martins, H. H. A., Manrich, A., Otoni, C. G., Carvalho, E. E. N. and Mattoso, L. H. C. 2020. Correlating emulsion characteristics with the properties of active starch films loaded with lemongrass essential oil. Food Hydrocolloids 100(10): 105-428.

Morais, W. A., Cavalcanti, I. M. F., Junior, F. H. X. and Maciel, M. A. M. 2017. Coencapsulation of *trans*-dehydrocrotonin and *trans*-dehydrocrotonin:hydroxypropyl-β-cyclodextrin into microparticles. Journal of the Brazilian Chemical Society 28(8): 1494-1505.

Musa, B. H. and Hameed, N. J. 2020. Study of the mechanical properties of polyvinyl alcohol/starch blends. Materials Today - Proceedings 20: 439-442.

Niazmand, R. and Razavizadeh, B. M. 2021. Active polyethylene films incorporated with β-cyclodextrin/ferula asafoetida extract inclusion complexes: Sustained release of bioactive agents. Polymer Testing 95: 107113.

Nisar, T., Wang, Z. C., Yang, X., Tian, Y., Iqbal, M. and Guo, Y. 2018. Characterization of citrus pectin films integrated with clove bud essential oil: Physical, thermal, barrier, antioxidant and antibacterial properties. International Journal of Biological Macromolecules 106: 670-680.

Panaitescu, D. M., Frone, A. N., Ghiurea, M. and Chiulan, I. 2015. Influence of storage conditions on starch/PVA films containing cellulose nanofibers. Industrial Crops and Products 70: 170-177.

Perumalla, A. V. S. and Hettiarachchy, N. S. 2011. Green tea and grape seed extracts - Potential applications in food safety and quality. Food Research International 44(4): 827-839.

Raeisi, S., Ojagh, S. M., Quek, S. Y., Pourashouri, P. and Salaün, F. 2019. Nano-encapsulation of fish oil and garlic essential oil by a novel composition of wall material: Persian gum-chitosan. LWT - Food Science and Technology 116: 108494.

Rajabinejad, H., Zoccola, M., Patrucco, A., Montarsolo, A., Chen, Y., Ferri, A., ... and Tonin, C. 2020. Fabrication and properties of keratoses/polyvinyl alcohol blend films. Polymer Bulletin 77(6): 3033-3046.

Song, W., Du, Y., Yang, C., Li, L., Wang, S., Liu, Y. and Wang, W. 2020. Development of PVA/EVA-based bilayer active film and its application to mutton. LWT - Food Science and Technology 133(5): 110109.

Sørensen, J. S., Ørnfeld-Jensen, O., Bøknæs, N., Mejlholm, O., Jessen, F. and Dalgaard, P. 2020. Thawed and chilled Atlantic cod (*Gadus morhua* L.) from Greenland - Options for improved distribution. LWT - Food Science and Technology 131: 109-473.

Srikhao, N., Kasemsiri, P., Ounkaew, A., Lorwanishpaisarn, N., Okhawilai, M., Pongsa, U., … and Chindaprasirt, P. 2021. Bioactive nanocomposite film based on cassava starch/polyvinyl alcohol containing green synthesized silver nanoparticles. Journal of Polymers and the Environment 29(2): 672-684.

Sun, C., Cao, J., Wang, Y., Chen, J., Huang, L., Zhang, H., ... and Sun, C. 2021. Ultrasound-mediated molecular self-assemble of thymol with 2-hydroxypropyl-β-cyclodextrin for fruit preservation. Food Chemistry 363(5): 130327.

Taghi Gharibzahedi, S. M., Razavi, S. H. and Mousavi, M. 2015. Optimal development of a new stable nutraceutical nanoemulsion based on the inclusion complex of 2-hydroxypropyl-β-cyclodextrin with canthaxanthin accumulated by *Dietzia natronolimnaea* HS-1 using ultrasound-assisted emulsification. Journal of Dispersion Science and Technology 36(5): 614-625.

Tao, T., Ding, C., Han, N., Cui, Y., Liu, X. and Zhang, C. 2019. Evaluation of pulsed light for inactivation of foodborne pathogens on fresh-cut lettuce: Effects on quality attributes during storage. Food Packaging and Shelf Life 21(5): 100358.

Tian, H., Yan, J., Rajulu, A. V., Xiang, A. and Luo, X. 2017. Fabrication and properties of polyvinyl alcohol/starch blend films: Effect of composition and humidity. International Journal of Biological Macromolecules 96: 518-523.

Wang, J., Chen, C. and Xie, J. 2022. Industrial crops and products loading oregano essential oil into microporous starch to develop starch / polyvinyl alcohol slow-release film towards sustainable active packaging for sea bass (*Lateolabrax japonicus*). Industrial Crops and Products 188: 115679.

Wang, Y., Yuan, C., Liu, Y. and Cui, B. 2021. Fabrication of kappa–carrageenan hydrogels with cinnamon essential oil/hydroxypropyl–β–cyclodextrin composite: Evaluation of physicochemical properties, release kinetics and antimicrobial activity. International Journal of Biological Macromolecules 170: 593-601.

Wong, L. W., Hou, C. Y., Hsieh, C. C., Chang, C. K., Wu, Y. S. and Hsieh, C. W. 2020. Preparation of antimicrobial active packaging film by capacitively coupled plasma treatment. LWT - Food Science and Technology 117(9): 108-612.

Xiao, Z., Hou, W., Kang, Y., Niu, Y. and Kou, X. 2019. Encapsulation and sustained release properties of watermelon flavor and its characteristic aroma compounds from γ-cyclodextrin inclusion complexes. Food Hydrocolloids 97(100): 105202.

Yang, W., Shi, W., Zhou, S., Qu, Y. and Wang, Z. 2019. Research on the changes of water-soluble flavor substances in grass carp during steaming. Journal of Food Biochemistry 43(11): 1-14.

Yıldırım-Yalçın, M., Sadıkoğlu, H. and Şeker, M. 2021. Characterization of edible film based on grape juice and cross-linked maize starch and its effects on the storage quality of chicken breast fillets. LWT - Food Science and Technology 142: 111012.

Yu, D., Zhao, W., Yang, F., Jiang, Q., Xu, Y. and Xia, W. 2021. A strategy of ultrasound-assisted processing to improve the performance of bio-based coating preservation for refrigerated carp fillets (*Ctenopharyngodon idellus*). Food Chemistry 345: 128862.

Yuan, C., Thomas, D. S., Hook, J. M., Qin, G., Qi, K. and Zhao, J. 2019a. Molecular encapsulation of *Eucalyptus staigeriana* essential oil by forming inclusion complexes with hydroxypropyl-β-cyclodextrin. Food and Bioprocess Technology 12(8): 1264-1272.

Yuan, L., Li, S., Zhou, W., Chen, Y., Zhang, B. and Guo, Y. 2019b. Effect of morin-HP-β-CD inclusion complex on anti-ultraviolet and antioxidant properties of gelatin film. Reactive and Functional Polymers 137(2): 140-146.

Zhang, W., Lv, X., Liu, Z. and Ni, L. 2022. The spoilage and adhesion inhibitory effects of *Bacillus subtilis* against *Shewanella* and *Pseudomonas* in large yellow croaker (*Pseudosciaena crocea*). Food Science and Technology 42: e02721.

Zong, L., Gao, H., Chen, C. and Xie, J. 2022. Effects of starch / polyvinyl alcohol active film containing cinnamaldehyde on the quality of large yellow croaker (*Pseudosciaena crocea*) proteins during frozen storage. Food Chemistry 389(11): 133065.